Material: Ferritic Steel: F82H
Property: Ni content (%) versus Micro-hardness (GPa)
Condition: Irradiated
Data: Experimental

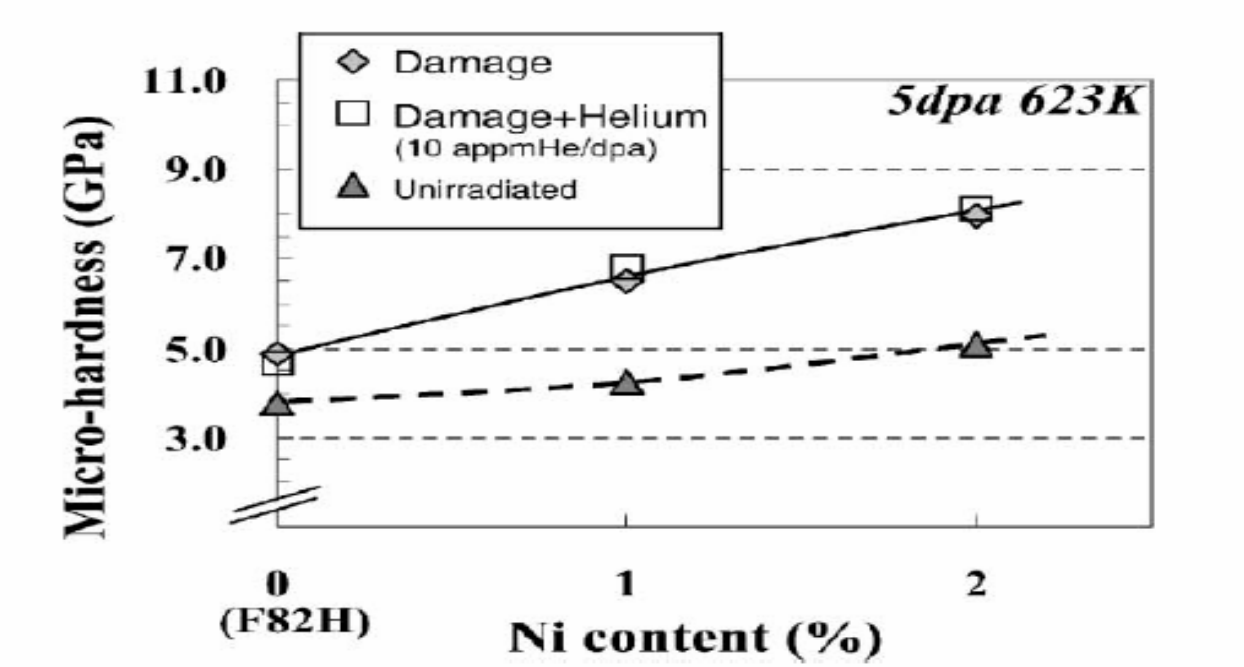

Fig. 4. Effect of helium on micro-hardness in F82H/Ni-doped F82H steel single/dual-beam irradiated at 623 K.

Source:
Journal of Nuclear Materials, 307-311, 2002, 260-265

Title of paper (or report) this figure appeared in:
Evaluation of hardening behavior of ion irradiated reduced activation ferritic/martensitic steel by an ultra-micro-indentation technique

Author of paper or graph:
M. Ando, H. Tanigawa, S. Jitsukawa, T. Sawai, Y. Katoh, A. Kohyama, K. Nakaruma, H. Takeuchi

Caption:
Effect of helium on micro-hardness in F82H/Ni-doped F82H steel single/dual-beam irradiated at 623 K.

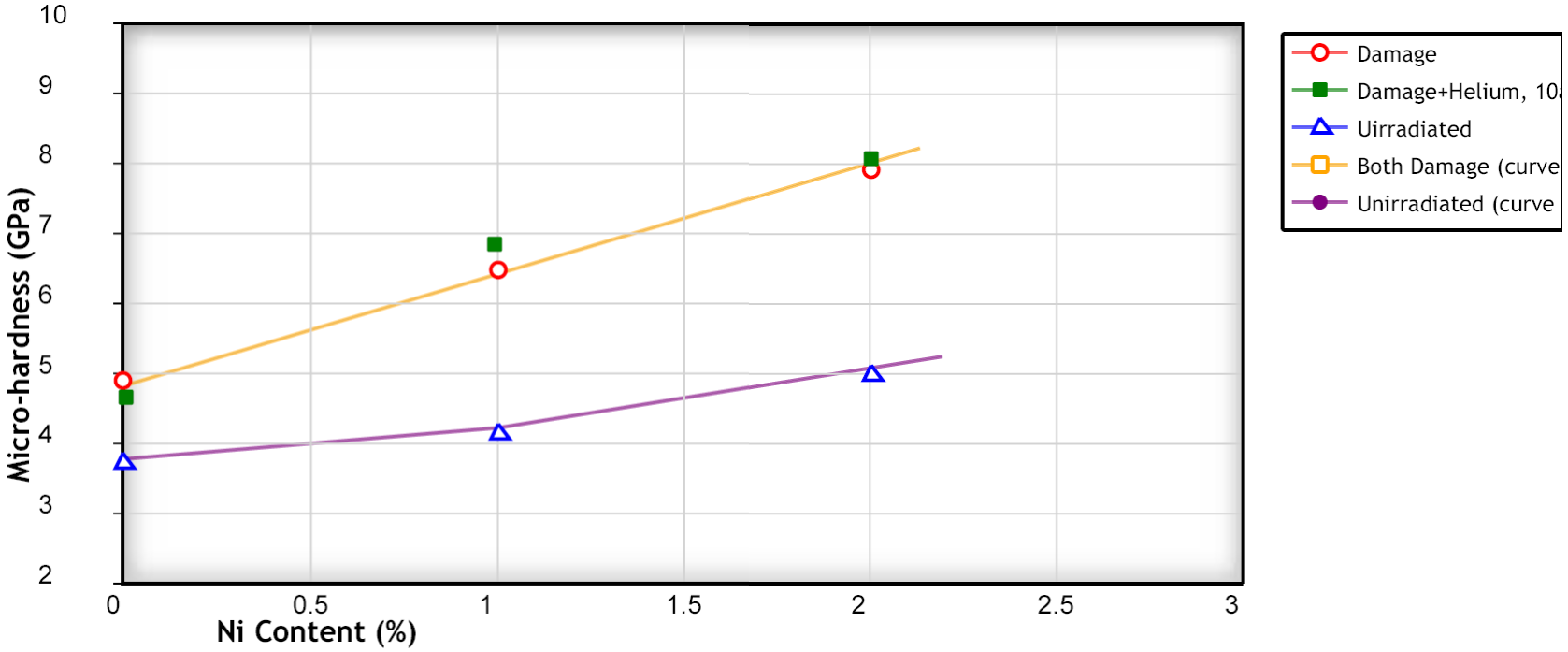

Effect of helium on micro-hardness in F82H/Ni-doped F82H steel single/dual-beam irradiated at 623 K.

Reference:

Author: *M. Ando, H. Tanigawa, S. Jitsukawa, T. Sawai, Y. Katoh, A. Kohyama, K. Nakaruma, H. Takeuchi*

Title: *Evaluation of hardening behavior of ion irradiated reduced activation ferritic/martensitic steel by an ultra-micro-indentation technique*

Source: *Journal of Nuclear Materials, 2002, Volume 307-311, Page 260-265*, [PDF]

View Data

Author Comments

Plot Format:

Y-Scale: ◉ linear ○ log ○ ln

X-Scale: ◉ linear ○ log ○ ln

ELSEVIER

Journal of Nuclear Materials 307–311 (2002) 260–265

journal of nuclear materials

www.elsevier.com/locate/jnucmat

Evaluation of hardening behaviour of ion irradiated reduced activation ferritic/martensitic steels by an ultra-micro-indentation technique

M. Ando [a,b,*], H. Tanigawa [a], S. Jitsukawa [a], T. Sawai [a], Y. Katoh [b], A. Kohyama [b], K. Nakamura [a], H. Takeuchi [a]

[a] *Institute of Advanced Energy, Kyoto University, Gokasho, Uji, Kyoto 611-0011, Japan*
[b] *Japan Atomic Energy Research Institute, Tokai 319-1195, Japan*

Abstract

The evaluation of the temperature dependence of irradiation hardening in a reduced activation ferritic/martensitic steel (RAFs), F82H (Fe–8Cr–2W–V–Ta) and Ni-doped (1%, 2%) F82H, was performed using single/dual-beam ion irradiation and ultra-micro-indentation technique. In analyzing the load–displacement curve, it was assumed that the elastic modulus did not exceed the original value due to irradiation-induced damage because micro-hardness was defined as a function of composite elastic modulus. Secondly, micro-structural evolution was characterized for irradiation conditions where significant changes in micro-hardness in RAFs were found. Finally, based on these results, the plastic deformation behavior of F82H steels with the irradiation hardening was investigated.

1. Introduction

One of the most critical issues in research and development of reduced activation ferritic/martensitic steels (RAFs) is the effect of defects and helium atoms generated simultaneously by 14 MeV neutron irradiation on mechanical properties. Irradiation hardening and embrittlement occur in RAFs, when they are neutron irradiated at lower temperatures (<673 K) [1,2], but the mechanism of irradiation-induced hardening is not clearly understood. Helium generation can be approximated by using mixed-spectrum neutron irradiation of ferritic steels doped with ^{10}B or ^{58}Ni, however, the mechanical evaluation of this effect is not necessarily simple [3,4]. Dual ion irradiation methods [5] provide a convenient way to simulate this condition, although the damaged volume is limited to the thin layer close to specimen surface. While ultra-micro-indentation tests can accurately measure the net hardness of this small surface volume, hardness is not a basic material property. Therefore, to better understand the mechanical properties from these results, detailed surface profile analysis around indents and micro-structure analysis of the indentation-induced plastic deformation zone needs to be performed [6,7].

The purpose of this study was to evaluate the hardening due to irradiation-produced defects and helium in F82H/Ni-doped F82H. Furthermore, the micro-structure following indentation-induced deformation was investigated to determine the barriers to moving dislocations.

2. Experimental procedure

The materials used in this study were F82H IEA heat, 1% Ni-doped and 2% Ni-doped F82H and modified

* Corresponding author. Address: Department of Fusion Engineering Research, Japan Atomic Energy Research Institute, 2-4 Shirakata Tokai-mura, Ibaraki-ken 319-1195 Japan. Tel.: +81-29 282 6146; fax: +81-29 282 5551.
E-mail address: andy@popsvr.tokai.jaeri.go.jp (M. Ando).

0022-3115/02/$ - see front matter
PII: S0022-3115(02)01250-3

Table 1
Chemical compositions and heat treatment conditions

	C	Cr	W	V	Ta	Mn	Si	Ni	P	Ti	S	N
F82H IEA heat[a]	0.090	7.71	1.95	0.16	0.02	0.16	0.11	–	0.002	–	0.0020	0.0060
1% Ni-doped F82H[b]	0.095	7.97	1.98	0.18	0.05	0.11	0.10	0.98	0.003	0.005	0.0022	0.0025
2% Ni-doped F82H[c]	0.097	7.92	1.99	0.19	0.06	0.11	0.10	1.97	0.003	0.005	0.0025	0.0036
Mod-F82H[d]	0.094	8.15	1.98	0.20	0.04	0.13	0.10	–	0.005	<0.001	0.0010	0.0017

[a] Normalized at 1313 K, 30 min, AC; tempered at 1023 K, 1 h, AC.
[b] Normalized at 1313 K, 30 min, AC; tempered at 1023 K, 1 h, AC.
[c] Normalized at 1313 K, 30 min, AC; tempered at 973 K, 20 h, AC.
[d] Normalized at 1313 K, 30 min, AC; tempered at 1013 K, 1.5 h, AC.

F82H (Mod-F82H). Mod-F82H steel is produced by hot rolling at low temperature (<1223 K). A detailed description of F82H IEA heat has been published elsewhere [8]. The chemical compositions and the heat treatment conditions are shown in Table 1. Disks of 3 mm diameter were punched out from the rolled sheet before ion irradiation. The disk specimens were electrolytically polished following mechanical polishing with 0.3 μm alumina powder.

The ion-beam irradiation experiment was carried out at the dual-beam for energy technology (DuET), facility of the University of Kyoto [9]. The atomic displacement damage was introduced by 6.4 MeV Fe^{3+} ions accelerated with a Tandetron tandem accelerator operating at 1.7 MeV. The irradiation temperature, displacement dose and displacement rate were 583–773 K, five displacement per atom (dpa) and 1×10^{-3} dpa/s, respectively. The helium-to-dpa ratio was 10 appmHe/dpa at the depth between 700 and 900 nm from irradiation surface with an energy degrader. The nominal displacement dose and the dose rate are the average over a 1.5 μm thick layer on the irradiated surface, as calculated by the TRIM-98 code [10] assuming a 40 eV average displacement threshold energy.

The irradiated specimens were then indentation-tested at loads in the range of 10–49 mN using an UMIS-2000 (CSIRO, Australia) ultra-micro-indentation testing system [11]. The direction of indentation was chosen to be parallel to the ion-beam axis, or normal to the irradiated surface. The indenter tip was triangular pyramid the Berkovich. Typically, indentations of the samples were made using at least 15×3 array of indents with about a 20 μm interval because the data scattering of micro-hardness in RAFs was larger than that of micro-hardness in solution annealed alloys and pure metals. The micro-indentation results were analyzed in the manner outlined by Oliver and Pharr [12] and Mencik and Swain [13].

Indentation micro-hardness, H and elastic modulus E^*, are determined from expressions

$$H = \frac{P}{A(h_c)}, \tag{1}$$

$$E^* = \frac{k}{\sqrt{A}} \frac{dP}{dh}, \tag{2}$$

where P is the indentation load and A, which is a function of contact depth (h_c), is the projected area of contact between the indenter and the specimen, k is a constant, and dP/dh is the slope of the load–displacement curve at the beginning of unloading. Generally, E^* denotes the composite modulus (that is, specimen + indenter). Contact depth is defined as

$$h_c = h - \varepsilon P_{max} \frac{dP}{dh}, \tag{3}$$

where h is the total penetration depth, ε is 0.75 theoretical value of which was obtained with Berkovich indenter and P_{max} is the maximum load.

The regions beneath the indents and regions away from the indents of the unirradiated and irradiated specimens were made into thin films using a Hitachi FB-2000A focused ion-beam (FIB) processing instrument with a micro-sampling system. The details of the FIB micro-sampling procedure have been explained elsewhere [14]. The foils were made so that they included the indentation axis. The ions used in this process were Gallium accelerated to 30 kV. The micro-structural examination was carried out using a JEOL JEM-2000FX transmission electron microscope (TEM) operating at 200 kV.

3. Results and discussion

3.1. Measurement of composite modulus E^*

Fig. 1 shows the results of the ultra-micro-indentation test for each ferritic steels at a load of 49 mN (penetration depth of about 800 nm). The composite modulus E^* is obtained from the slope of the load–displacement curve at the beginning of unloading. Ideally, the modulus E^* should be a constant for the same material [7]. Therefore, in this micro-indentation analysis, the micro-indentation hardness, which approximately

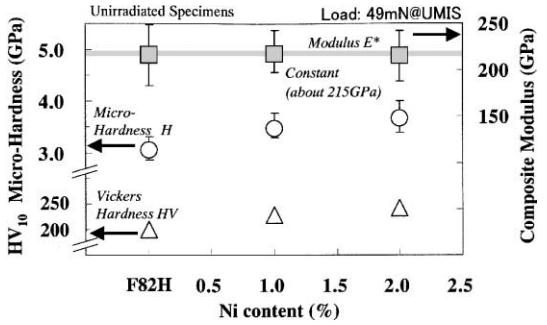

Fig. 1. Relationship between micro-indentation hardness, micro-Vickers, composite modulus and Ni content in unirradiated F82H/Ni-doped F82H.

corresponded to the average modulus in Fig. 1, was selected. As a result, the 2% Ni-doped F82H had the largest micro-hardness of all. This micro-hardness variation is qualitatively consistent with the Vickers hardness results [15]. Because the increase in the Vickers hardness can be correlated with the increase in yield stress [16], it is suggested that the micro-indentation hardness shows yield stress change in single-phase micro-structure.

3.2. Temperature dependence of radiation hardening

Micro-indentation tests were performed on each of the ferritic steels at loads which enabled penetration to about 300 nm. The elastic modulus nearly becomes constant in the case of the penetration by more than about 300 nm in RAFs. Furthermore, the indentation-induced deformation region approximately includes the irradiation-induced damage range in an austenitic model alloy [6]. Fig. 2 shows the temperature dependence of

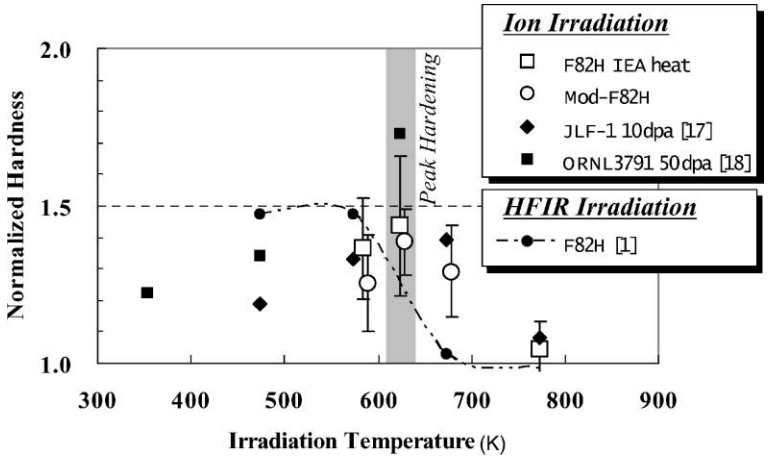

Fig. 2. The irradiation temperature dependence of normalized micro-hardness of the F82H.

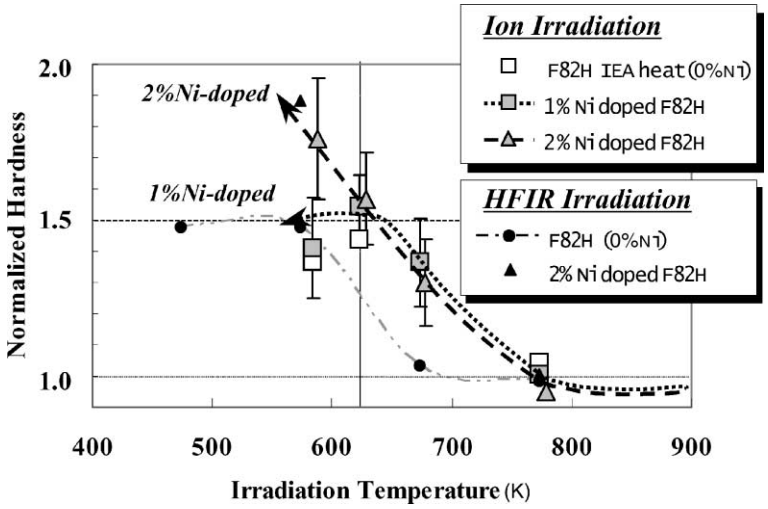

Fig. 3. The irradiation temperature dependence of normalized micro-hardness of the Ni-doped F82H steel.

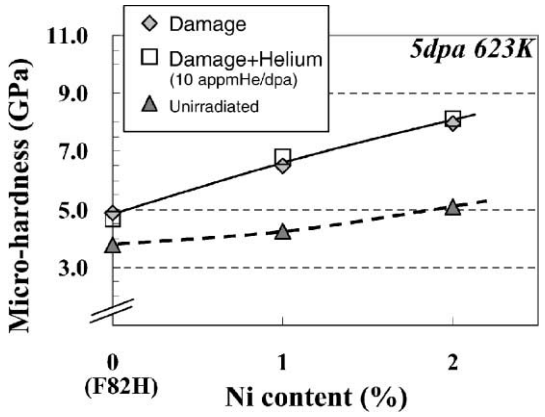

Fig. 4. Effect of helium on micro-hardness in F82H/Ni-doped F82H steel single/dual-beam irradiated at 623 K.

normalized hardness in each of the ferritic steels. Irradiation hardening was found in all irradiated specimens. For the F82H ferritic steel, the peak normalized hardness change was about 40% at 623 K, while little irradiation-hardening was measured for the specimen irradiated at 773 K. This temperature dependence agrees approximately with the results of micro-hardness evaluation of JLF-1 steels irradiated at the HIT Facility [17], and with nano-indentation results for ORNL3791 steels irradiated up to 50 dpa at ORNL [18].

3.3. Irradiation hardening in Ni-doped F82H

Fig. 3 shows that the ion-irradiated 2% Ni-doped F82H exhibited hardening over 80% at 583 K. This result agrees qualitatively with irradiation behavior of 2% Ni-doped F82H irradiated in HFIR. In contrast, the hardening of the ion-irradiated 1% Ni-doped F82H was nearly equal to that of F82H steels ion-irradiated at 583 K. For the specimens which exhibited large irradiation-induced hardening, the micro-hardness data scatter was larger than for unirradiated specimen. This scatter in micro-indentation hardness is believed to have been caused by the effects of inhomogeneous dislocation micro-structure, and anisotropic martensitic lath structures. Tanigawa et al. [19] reported that a clear difference in swelling was observed by comparing, in a depth profile, swelling on different lathes in high-fluence dual-ion irradiated RAFs. Fig. 4 shows the effect of helium co-implantation on Ni contents in Ni-doped F82H irradiated at 623 K. The helium-to-dpa ratio was 10 appmHe/dpa. The indentation condition was similar at a penetration depth of 300 nm. As a result, the irradiation hardening was slightly less in the single ion-irradiated specimen in which only displacement damage was

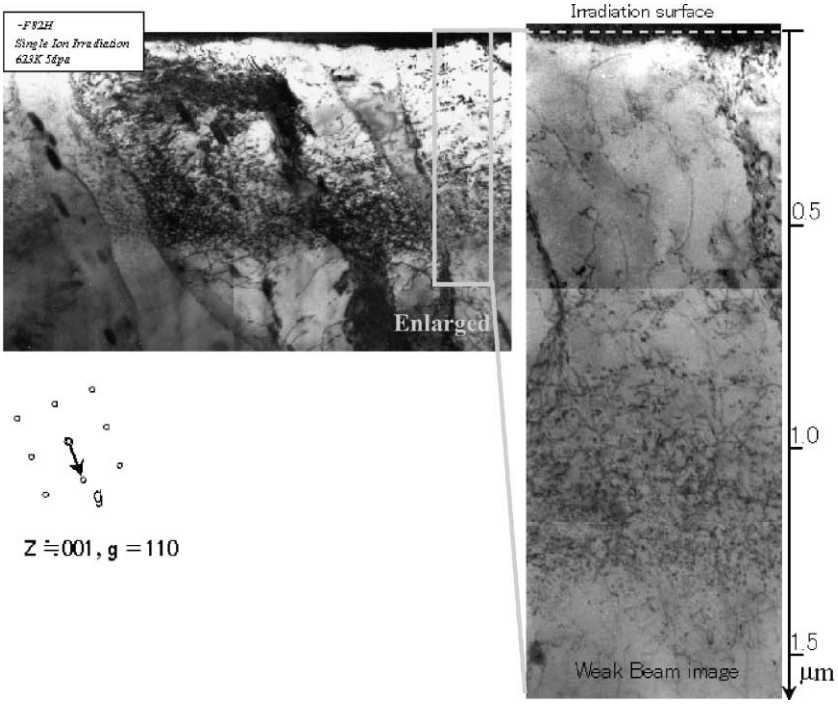

Fig. 5. Cross-sectional TEM image in a single ion-irradiated F82H steel at 623 K.

induced. Therefore, it can be concluded that there is no effect of co-implanted helium up to 50 appm on irradiation hardening.

3.4. Micro-structural observation

Fig. 5 shows an example of the micro-structure in the specimen exhibiting the most hardening. This image is a cross-sectional TEM bright field image in single ion-irradiated F82H (623 K, 5 dpa). The zone-axis is near $z = [0\,0\,1]$, $g = [1\,1\,0]$ (two-beam method). In both the unirradiated and irradiated regions, the micro-structure was a typical lath martensitic structure. Large precipitates ($M_{23}C_6$ carbides) were observed in the matrix and on grain boundaries. In depth range 850–1200 nm, micro-structural features included a large population of fine dislocation loops (with a diameter of about 10 nm), dot-like defects (with diameter <5 nm) and network of dislocations. However, a few loops and network dislocations were observed on the surface side (up to 500 nm). These fine loops were mainly $a_0/2\langle 1\,1\,1\rangle$ type loops at depth ranging from 850 to 1200 nm. The number density and the average diameter of these loops were $0.9 \times 10^{23}/m^3$ and 8.5 nm, respectively. Some dislocation loops were arranged along dislocation lines. These features were similar to the micro-structures in RAFs irradiated in HFIR [20,21]. It should be noted that the distribution of irradiation-induced defects was not homogeneous in the depth direction, suggesting that the formation of fine dislocation loops, which caused a large hardening, required a certain threshold damage level.

Fig. 6 shows a cross-sectional TEM bright field image of the region beneath an indent with $z \fallingdotseq [\bar{1}\,1\,1]$, $g = [1\,1\,0]$ conditions (two-beam method). As a result of the 11 mN (1.12 gf) indentation, the fine dislocation loops disappeared from the region beneath the indent. Therefore, the major contributor to the irradiation hardening is likely to be these fine dislocation loops. Detailed investigation of these defect interactions will be performed in future studies.

4. Summary

This work was performed to evaluate irradiation-induced hardening due to ion-irradiation-produced defects and helium in F82H/Ni-doped F82H. The main results can be summarized as follows:

(1) The composite modulus E^* remained constant for unirradiated specimens. For evaluation of micro-indentation hardness, the average modulus, which approximately corresponded to this modulus E^* was selected.
(2) For F82H ferritic steel, the peak of normalized hardness change was about 40% at 623 K, while little irradiation-hardening was measured for the specimen irradiated at 773 K. On the other hand, the 2% Ni-doped F82H exhibited hardening over 80% at 583 K. However, the hardening of the 1% doped-Ni F82H was nearly equal to that of undoped F82H steels ion-irradiated at 583 K. Furthermore, co-implanted helium up to 50 appm in F82H and Ni-doped F82H did not cause additional hardening.
(3) A large amount of fine dislocation loops, dot-like defects and network dislocations were observed in the ion irradiated F82H which appeared to have caused most of the hardening. The major contributors to the irradiation hardening are likely to be the fine dislocation loops.
(4) The distribution of irradiation-induced defects was observed not to be homogeneously in the depth di-

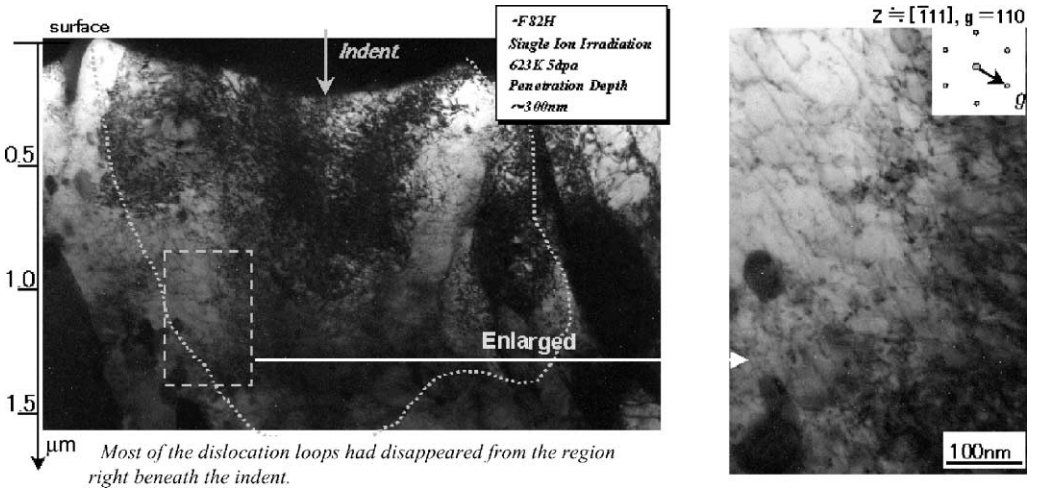

Fig. 6. Micro-indented micro-structure of ion-irradiated F82H at 623 K.

rection, which is in contrast to an irradiated austenitic model alloy. This suggests that the formation of fine dislocation loops, which caused the large hardening, required a certain threshold damage level.

(5) Fine dislocation loops disappeared in the region beneath the indent compared to the region away from the indent.

Acknowledgements

The authors would like to thank the members of Radiation Effect Analysis Laboratory in JAERI, for their insightful comments on this paper. It is a pleasure to acknowledge the hospitality of the members of the Hot Laboratory at JAERI.

References

[1] A. Hishinuma, A. Kohyama, R.L. Klueh, D.S. Gelles, W. Dietz, K. Ehrlich, J. Nucl. Mater. 258–263 (1998) 193.
[2] K. Shiba, A. Hishinuma, J. Nucl. Mater. 283–287 (2000) 474.
[3] R. Kasada, A. Kimura, H. Matsui, M. Narui, J. Nucl. Mater. 258–263 (1998) 1199.
[4] R.L. Klueh, M.A. Sokolov, K. Shiba, Y. Miwa, J.P. Robertson, J. Nucl. Mater. 283–287 (2000) 478.
[5] Y. Kohno, K. Asano, A. Kohyama, K. Hasegawa, N. Igata, J. Nucl. Mater. 141–143 (1986) 794.
[6] M. Ando, Y. Katoh, H. Tanigawa, A. Kohyama, T. Iwai, J. Nucl. Mater. 283–287 (2000) 423.
[7] H. Tanigawa, M. Ando, S. Jitsukawa, Y. Katoh, A. Kohyama, T. Iwai, Investigation of Hardness Changes on Helium-Ion Implanted Iron by Ultra-micro-hardness Testing ASTM STP1418, in press.
[8] K. Shiba, A. Hishinuma, A. Tohyama, K. Kasamura, Properties of Low Activation Ferritic Steel F82H IEA Heat, JAERI-Tech 97-038, JAERI, 1997.
[9] A. Kohyama, Y. Katoh, M. Ando, K. Jimbo, Fus. Eng. Des. 51&52 (2000) 789.
[10] J.P. Biersack, L.G. Haggmark, Nucl. Instrum. and Meth. 174 (1980) 257.
[11] M. V. Swain, Characterisation of materials using ultra-micro-indentation tests with pointed and spherical indenters, CSIRO.
[12] W.D. Oliver, G.M. Pharr, J. Mater. Res. 7 (1992) 1564.
[13] J. Mencik, M.V. Swain, Mater. Forum 18 (1994) 277.
[14] T. Hirose, H. Tanigawa, M. Ando, A. Kohyama, Y. Katoh, S. Jitsukawa, Mater. Trans. 42 (3) (2001) 389.
[15] Sawai et al., these Proceedings.
[16] G.E. Lucus, G.R. Odette, R. Maiti, Sheckherd, Influence of Radiation on Material Properties, ASTM STP 956, ASTM, Philadelphea, PA, 1987.
[17] Y. Katoh, H. Tanigawa, T. Muroga, T. Iwai, A. Kohyama, J. Nucl. Mater. 271&272 (1999) 115.
[18] E.H. Lee, J.D. Hunn, G.R. Rao, R.L. Klueh, L.K. Mansur, J. Nucl. Mater. 271&272 (1999) 385.
[19] H. Tanigawa, M. Ando, Y. Katoh, A. Kohyama, T. Hirose, H. Sakasegawa, T. Iwai, J. Nucl. Mater., submitted for publication.
[20] N. Hashimoto, J.P. Robertson, A.F. Rowcliffe, Y. Miwa, K. Shiba, DOE/ER-0313/25, FRM Semiannual Prog. Rept., 1998.
[21] E. Wakai, N. Hashimoto, K. Shiba, T. Sawai, J.P. Robertson, R.L. Klueh, DOE/ER-0313/25, FRM Semiannual Prog. Rept., 1998.